A Charge Density Analysis of Cationic and Anionic Hydrogen Bonds in a "Proton Sponge" Complex

Paul R. Mallinson,*,† Krzysztof Woźniak,‡ Garry T. Smith,†,§ and Kirsty L. McCormack†

Contribution from the Chemistry Department, University of Glasgow, Glasgow G12 8QQ, UK, and Chemistry Department, University of Warsaw, 02-093 Warszawa, ul. Pasteura 1, Poland

Received June 12, 1997. Revised Manuscript Received September 19, 1997[⊗]

Abstract: The charge density distribution in crystals of the 1,2-dichloro hydrogen maleate salt formed by 1,8-bis-(dimethylamino)naphthalene (DMAN) has been obtained by high-resolution X-ray and neutron diffraction at 100 K. The asymmetric $[Me_2N-H\cdots NMe_2]^+$ hydrogen bond in the monoprotonated cation is characterized by nonlinear interaction lines, constrained by crystallographic symmetry to lie in the plane of the DMAN molecule; the critical point situated between the proton and the acceptor nitrogen atom lies in a region of positive Laplacian of the charge density. The lone pair of this nitrogen atom is polarized in the direction of the hydrogen bond. The N−C(aromatic) bond paths are slightly curved. Magnitudes of the charge density at critical points in covalent and hydrogen bonds within both ions are compared with values obtained from an *ab initio* MO single point calculation for a cation−anion pair. Properties of the charge density in a number of weak C−H···O interionic interactions are found to be systematically related to the donor−acceptor separation. A series of *ab initio* calculations on a model formate ion−benzene complex shows that the density at C−H···O hydrogen bond critical points is systematically lower than the density of the superposed moieties, but by an amount that is on the threshold of current experimental measurements analyzed with multipole-based models.

Introduction

Proton sponges are organic diamines with unusually high basicity. The very first proton sponge, 1,8-bis(dimethylamino)-naphthalene (DMAN) was reported in 1968.[1] This compound has a basicity *ca.* 10 million times higher ($pK_a = 12.1$) than other similar organic amines as for example aniline ($pK_a = 5.1$). With mineral or organic acids proton sponges form very stable ionic complexes containing strong, charge supported, intramolecular $[R_2N-H\cdots NR_2]^+$ hydrogen bonding. Properties of such hydrogen bonds are used in discussion of the role of hydrogen bonding in low energetic enzymatic catalysis.[2,3] The charge in these strong, charged hydrogen bonds has been studied theoretically at the Hartree−Fock level[4−6] but not at all experimentally.

1,8-Diaminonaphthalenes show a wide range of basic strengths, depending on the substituents in the amine groups, with observed pK_a values ranging up to 16.3.[7] Some data for typical "proton sponge" compounds are given in Table 1. The ammonium ion, for comparison, has $pK_a = 9.25$. Proton sponges and their complexes have attracted considerable interest, giving rise to over 70 structural and 100 spectroscopic papers. Among others the DMAN structure itself has been intensively studied by means of theoretical methods,[4] X-ray[8,9] and neutron diffraction,[10] solid-state NMR,[11,12] and NQR spectroscopies.[9,13,14] The older results regarding proton sponges are nicely summarised in three important review papers by Alder,[15] Staab and Saupe,[7] and Llamas-Saiz and co-workers.[16]

Table 1. Basicities of Some Substituted 1,8-Diaminonaphthalenes

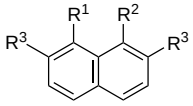

R^1	R^2	R^3	pK_a
NH_2	NH_2	H	4.61
NHMe	NHMe	H	5.61
NMe_2	NHMe	H	6.43
NMe_2	NMe_2	H	12.1
NEt_2	NEt_2	H	12.7
NMe_2	NMe_2	OMe	16.1
NEt_2	NEt_2	OMe	16.3

* Address correspondence to this author. e-mail: paul@chem.gla.ac.uk. Fax +44(141) 330 4888.
† University of Glasgow.
‡ University of Warsaw.
§ Present address: Chemistry Department, Queen's University, Kingston, Ontario K7L 3N6, Canada.

⊗ Abstract published in *Advance ACS Abstracts,* November 15, 1997.

(1) Alder, R. W.; Steele, W. R. S.; Winterman, D. R. *J. Chem. Soc., Chem. Commun.* **1968**, 723.
(2) Cleland, W. W.; Kreevey, M. M. *Science* **1995**, *269*, 104.
(3) Frey, P. A. *Science* **1995**, *269*, 104.
(4) Platts, J. A.; Howard, S. T.; Woźniak, K. *J. Org. Chem.* **1994**, *59*, 4647.
(5) Howard, S. T.; Platts, J. A.; Alder R. W. *J. Org. Chem.* **1995**, *60*, 6085.
(6) Platts, J. A.; Howard, S. T. *J. Org. Chem.* **1996**, *61*, 4480.
(7) Staab, H. A.; Saupe, T. *Angew. Chem., Int. Ed. Engl.* **1988**, *27*, 865.
(8) Einspahr, H.; Robert, J-B.; Marsh R. E.; Roberts, J. D. *Acta Crystallogr.* **1973**, *B29*, 1611.
(9) Woźniak, K.; He, H.; Klinowski, J.; Nogaj, B.; Lemanski, D.; Hibbs, D.; Hursthouse M.; Howard, S. T. *J. Chem. Soc., Faraday Trans.* **1995** *91*, 3925.
(10) Woźniak, K.; Wilson, C. C. in preparation.
(11) Woźniak, K. *J. Mol. Struct.* **1996**, *374*, 227. Grech, E.; Stefaniak, L.; Ando, I.; Yoshimizu, H.; Webb, G. A. *Bull. Chem. Soc. Jpn.* **1991**, *64*, 3761. Woźniak, K.; He, H.; Klinowski, J.; Jones, W.; Barr, T. L.; Hardcastle. S. *J. Phys. Chem.* **1996**, *100*, 11408.
(12) Woźniak, K.; He, H.; Klinowski, J.; Barr, T. L.; Milart, P. *J. Phys. Chem.* **1996**, *100*, 11420.
(13) Nogaj, B.; Woźniak, K.; Lemanski, D.; Ostafin, M.; Grech. E. *Solid State NMR* **1995**, *4*, 187.
(14) Stephenson, D.; Smith, J. A. S. *Proc. R. Soc. London* **1988**, *A416*, 149.
(15) Alder, R. W. *Chem. Rev.* **1989**, *89*, 1215.
(16) Llamas-Saiz, A. L.; Foces-Foces, C.; Elguero, J. *J. Mol. Struct.* **1994**, *328*, 297.

S0002-7863(97)01940-9 CCC: $14.00

Platts *et al.*[4] located the nitrogen lone pair in *ab initio* MO calculations on a series of amines. Lone pairs appear as (3,−3) critical points in the negative Laplacian distribution $-\nabla^2\rho$ of the charge density. Comparison of the values of ρ and $\nabla^2\rho$ at the lone pair position and the distance of the lone pair from the nucleus shows no obvious trend in these properties. It seems that the unusual basic strength of DMAN is not attributable to unusual characteristics of the N lone pair. This has been explained in terms of a "proximity effect" of the two amino groups.[7,15,16] This was also later reported by Peräkylä.[17]

Here we report the first example of an experimental charge density analysis of a proton sponge complex—the crystalline acid salt formed by DMAN with 1,2-dichloromaleic acid ($ClMH_2$). The DMAN molecule in the crystalline complex is protonated, and the naphthalene nucleus lies in a crystallographic mirror plane. The 1,2-dichloro hydrogen maleate anion lies in the same mirror plane, giving rise to a number of relatively weak C−H···O interactions. The salt contains two strong, asymmetric hydrogen bonds $[Me_2N-H\cdots NMe_2]^+$ and $[O-H\cdots O]^-$.[18]

The presence of both cationic and anionic hydrogen bonding and weak C−H···O hydrogen bonds make this DMAN−maleic acid complex an ideal candidate for an experimental study. The X-ray and neutron diffraction structures of the complex have already been published.[19,20] In this paper we concentrate on the charge density analysis of strong ionic $[N-H\cdots N]^+$ and $[O-H\cdots O]^-$ hydrogen bonds in the $DMANH^+$ cation and the $ClMH^-$ anion (both of which appear to be asymmetric[20]) and, on the other hand, on a series of the weakest C−H···X interactions where X stands for O or Cl atoms.

Experimental Section

Crystals of the acid salt formed by DMAN with 1,2-dichloromaleic acid are colorless prisms. Single-crystal, high-resolution X-ray diffraction data were collected on a CAD4 diffractometer with use of graphite-monochromated Mo Kα radiation. The crystal was cooled by a stream of cold nitrogen gas from an Oxford Cryosystems Cryostream cooler. Data reduction was carried out with the DREAM suite of programs,[21] including an analytical absorption correction computed with ABSORB.[22] The intensities of standard reflections were fitted to cubic polynomials, which were used for scaling the data. Corrections were made for absorption by the crystal, but not for thermal diffuse scattering. The range of corrections, agreement factor for the averaging of equivalent reflections, crystal data, and other experimental details are summarized in Table 2.

Multipole Refinement. The space group requires both cation and anion in the crystal to have point symmetry C_s.[19] The refinement minimized the function $\sum w(|F_o| - K|F_c|)^2$, where $w = 1/\sigma^2(F) = 4F^2/\sigma^2(F^2)$ and $\sigma^2(F^2) = \sigma^2_{counting}(F^2) + P^2F^4$. The instrumental instability factor P was estimated from errors in the time-dependent scaling polynomials and the fluctuations of the standards. Anisotropic temperature factors were used to describe the thermal motion of all atoms. For hydrogen atoms, positional and thermal parameters obtained from refinement with neutron diffraction data were used. Scattering factors for C, H, N, O, and Cl were derived from wave functions tabulated in ref 23. The program XDLSM of the package XD[24] was used for the multipole refinement. The rigid pseudoatom model[25] has become the established tool in the extraction of the charge density from experimental data; a detailed account of the technique is given in ref 26. The electron density $\rho(\mathbf{r})$ in the crystal is described by a sum of aspherical "pseudoatoms" with nuclear positions $\{\boldsymbol{R}_j\}$

$$\rho(\mathbf{r}) = \sum_j \rho_j(\mathbf{r} - \mathbf{R}_j) \tag{1}$$

In XDLSM the pseudoatom density has the form

$$\rho_j(\mathbf{r}_j) = P_c\rho_c(r_j) + \kappa'^3\, P_v\rho_v(\kappa' r_j) + \sum_{l=0}^{l_{max}} \sum_{m=-l_{max}}^{+l_{max}} \kappa''^3\, P_{lm} R_l(\kappa'' r_j) d_{lmp}(\theta_j,\phi_j) \tag{2}$$

where $\boldsymbol{r}_j = \boldsymbol{r} - \boldsymbol{R}_j$. Each pseudoatom is described by three components. The first, $P_c\rho_c$ describes the core density. The core population P_c is fixed (at 2 for first-row atoms), and ρ_c is the spherically-averaged Hartree−Fock core density for the atom. The second term describes the spherical part of the valence density. This is usually also obtained from the Hartree−Fock wave function; κ' is an expansion-contraction coefficient which allows the radial density to become more or less diffuse, being varied in the least-squares refinement along with the valence population P_v. The final, double summation term describes the deviation of the pseudoatom density from sphericity. This is represented by deformation functions taking the shape of density-normalized spherical harmonics d_{lmp} of order l oriented with index m and sign p.[27] The radial term for the deformation functions can take

Table 2. Experimental Data for the Complex of 1,8-Bis(dimethylamino)naphthalene with 1,2-Dichloromaleic Acid

formula	$[C_{14}H_{19}N_2]^+\,[C_4HCl_2O_4]^-$
mol wt	399.3
space group (orthorhombic)	Pmna
temp/*K*	100(5)
unit cell dimens/Å	
a	18.078(2)
b	6.977(1)
c	14.356(3)
V /Å^3	1810.7(6)
Z	4
D_c/g cm^{-3}	1.46
cryst dimens/mm	0.4 × 0.2 × 0.2
abs coeff/cm^{-1}	3.8
range of corrections for abs by crystal	0.906−0.939
radiation	Mo *K*α; λ = 0.7107 Å
scan type	$\theta-2\theta$
$\sin(\theta)/\lambda_{max}$/Å^{-1}	1.102
(*hkl*) lower limit-upper limit	−39 39; −14 14; −30 30
time period/h	574
no. of standard reflcns	6($22\bar{1}$, 111, 002, 060, $2\bar{2}\bar{1}$, $41\bar{2}$)
no. of reflcns measd	17224
no. of symmetry-independent reflcns	4931
no. of $I > 2\sigma(I)$ reflcns	3922
no. of symmetry-related and repeated reflcns	4826
agreement factor $R = \sum\|I - \bar{I}\|/\sum I$	0.029
refined on	*F*
R	0.0241
R_w	0.0244
S	0.925
N_{obs}/N_{var}	8.3
weighting scheme	$w = 1/\sigma^2(F) = 4F^2/\sigma^2(F^2)$
positional and thermal param for H atoms taken from refinement with neutron data	$\sigma^2(F^2) = \sigma^2_{counting}(F^2) + P^2F^4$

(17) Peräkylä, M. J. *J. Org. Chem.* **1996**, *61*, 7420.
(18) Woźniak, K.; He, H.; Klinowski, J.; Grech, E. *J. Phys. Chem.* **1995**, *99*, 1403.
(19) Woźniak, K.; He, H.; Klinowski, J.; Jones, W.; Barr, T. L. *J. Phys. Chem.* **1995**, *99*, 14667.
(20) Woźniak, K.; Wilson, C. C.; Knight, K. S.; Jones, W.; Grech, E. *Acta Crystallogr.* **1996**, *B52*, 691.
(21) Blessing, R. H. *J. Appl. Crystallogr.* **1989**, *22*, 396 and references cited therein.
(22) DeTitta, G. *Computer program ABSORB*; Medical Foundation of Buffalo, U.S.A., 1984.
(23) Clementi, E.; Roetti, C. *At. Data Nucl. Data Tables* **1974**, *14*, 177.
(24) Koritsanszky, T.; Howard, S. T.; Richter, T.; Mallinson, P. R.; Su, Z.; Hansen, N. K. *XD, a computer program package for multipole refinement and analysis of charge densities from X-ray diffraction data*, 1995.
(25) Stewart, R. F. *Acta. Crystallogr.* **1976**, *A32*, 565.
(26) Coppens, P. *X-Ray Charge Densities and Chemical Bonding*; Oxford University Press: IUCr Texts on Crystallography No. 4, 1997.

the form of a normalized Slater function $R_l(r) = r^{n_l}e^{-\kappa''\zeta r}$, with an expansion-contraction parameter κ'' again in place to alter the radial dependance of the functions. The n_l and ζ are taken from reference.[27] Alternatively, Hartree−Fock radial functions may be used in the deformation term. The deformation functions with $l \geq 1$ are defined with respect to Cartesian axes which are local to each pseudoatom. This makes possible the description of any chemical or crystallographic symmetry in the molecule.

XDLSM provides an overall neutrality constraint, which may be expressed as a constraint on the monopole charges q_j:

$$\sum_j (Z_j - P_c - P_v) = \sum_j q_j = 0 \qquad (3)$$

Further, specified groups of atoms may be constrained so that each has a particular net charge. The population parameters are on an absolute scale, and an overall scale factor is usually refined to scale the calculated to the observed structure factors.

In the multipole refinement, the expansion was truncated at the octapole level ($l_{max} = 3$) for carbon and nitrogen atoms, and at the dipole level ($l_{max} = 1$) for all hydrogen atoms except strongly H-bonded H1nn and H1oo, for which quadrupole functions ($l_{max} = 2$) were included. For all other hydrogen atoms a single, bond-directed dipole was used, and in each methyl group the three hydrogen atoms were constrained to have the same multipole coefficients so as to help keep the observations/variables ratio at a reasonable level. Hexadecapole functions ($l_{max} = 4$) were included for the oxygen and chlorine atoms. The space group symmetry restricts the allowed multipoles d_{lm} for atoms on the mirror plane (all except those of the methyl groups) such that only combinations with (even l, even m) and (odd l, odd m) are non-zero. Separate κ',κ'' were employed for aromatic C, methyl C, anionic C, and amino-bonded C, N, O, Cl, and H. Their values were allowed to vary, except those relating to H, which were fixed at 1.2, an average value found from theoretical models.[28] Highly contracted κ'' values (1.6) for Cl were obtained in the multipole refinement. Variation of the model by forcing equality of their multipole populations did not change this result, for which we find no obvious explanation.

Coordinates and temperature factors for the hydrogen atoms were fixed at the values obtained from the neutron diffraction experiment already mentioned.[20] For crystal structures analyzed by both X-ray and neutron diffraction the thermal parameters of the non-H atoms are sometimes found to differ significantly.[21] A comparison between thermal parameters from the neutron and an earlier X-ray experiment for this particular compound was made in ref 20. A linear dependance was found between U_{eq} values for corresponding non-H atoms, which could be related to the ratio of the measurement temperatures. However, in the present X-ray study the temperature was the same as in the neutron experiment. There is nevertheless a systematic difference such as discussed by Blessing.[21] We opted to refine the non-H atom thermal parameters with the X-ray data, rather than applying a modifying factor to the neutron values.

A charge constraint was applied such that the cation and anion charges are +1 and −1 e. Refinement without this charge constraint led to ionic charges +0.9 and −0.9 e. These are not significantly different from the formal charges and the constraint was applied in the final refinement.

Results

Details of the final *R* factors and goodness of fit for the 4826 reflections used in the multipole refinement are given in Table 2. Atom labeling is shown in Figure 1. Residual densities in the planes of the cation and anion are shown in Figure 2.

Parts a and b in Figure 3 show the Laplacian distributions in these planes found experimentally, computed with the program XDPROP of the XD package.[24] This was used also to obtain a critical point (CP) analysis for the bonds within the cation and anion, and for intermolecular hydrogen bonds. The bond paths (lines along which charge is concentrated, and on which the CPs are situated) are depicted in Figure 4, together with the charge densities ρ_b calculated at the bond critical points. In addition to the strong $[Me_2N-H\cdots NMe_2]^+$ and $[O-H\cdots O]^-$ bonds within the cation and anion there are a number of relatively weak interionic [C−H···O] bonds. These are listed in Table 3, with their geometrical parameters calculated from the nuclear positions refined with neutron diffraction data.

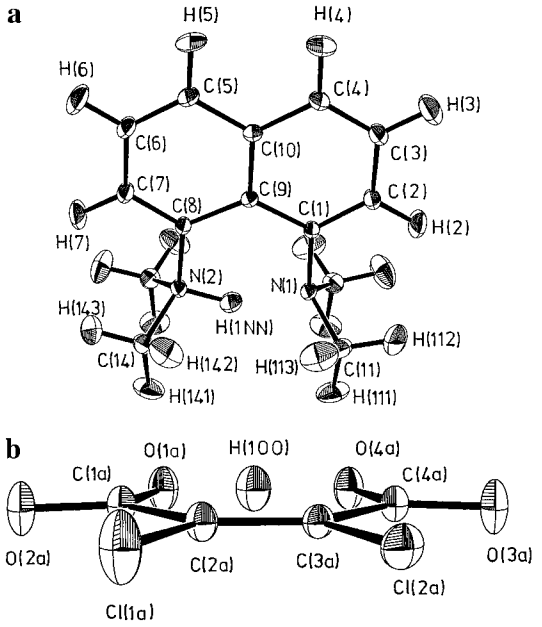

Figure 1. Anisotropic displacement ellipsoids for (a) the cation and (b) the anion, drawn at 50% probability, showing the labeling of the atoms.

Hirshfeld's rigid bond test[30] was applied to the thermal parameters obtained from the refinement. It is supposed that the relative vibrational motion of a pair of covalently bonded atoms has an effectively vanishing component in the direction of the bond. If $z^2_{A,B}$ denotes the mean square displacement amplitude of atom A in the direction of atom B, then for every covalently bonded pair of atoms A and B

$$\Delta_{A,B} = z^2_{A,B} - z^2_{B,A} = 0$$

Two bonds have $\Delta_{A,B}$ values slightly greater than Hirshfeld's upper limit of 0.001 Å^2 for atoms at least as heavy as carbon, *viz.* C8−C9 0.0011 Å^2 and O2a−C1a 0.0016 Å^2.

For comparison with the experimental charge density distribution an *ab initio* wave function has been used to compute a reference theoretical distribution. The Laplacian maps derived from this with AIMPAC[31] are shown in Figure 3, parts b and d. Values of ρ_b are shown in Figure 4 for both cation and anion, along with the experimental values. The *ab initio* MO calculation used a 6-311G** basis set at the Hartree−Fock level of theory and included a complete, therefore neutral, cation−anion pair situated in a plane of symmetry. The single point calculation of the wave function was carried out with GAUSSIAN94,[32] with nuclear positions obtained from the neutron diffraction experiment.[20]

(27) Hansen N. K.; Coppens, P. *Acta Crystallogr.* **1978**, *A34*, 909.
(28) Howard, S. T. Personal communication.
(29) Blessing, R. H. *Acta Crystallogr.* **1995**, *B51*, 816.
(30) Hirshfeld, F. L. *Acta Crystallogr.* **1976**, *A32*, 239.
(31) Biegler-König, F. W.; Bader, R. F. W.; Tang, T. H. *J. Comput. Chem.* **1982**, *3*, 317.

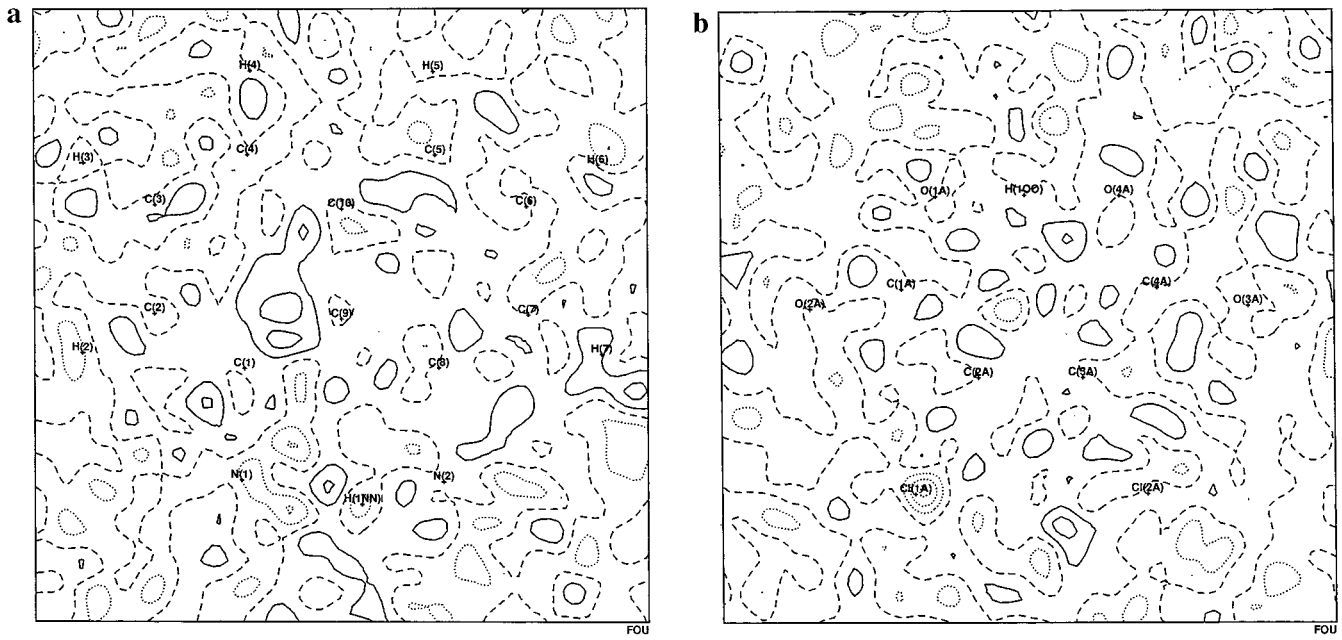

Figure 2. Residual density in the plane of (a) the cation and (b) the anion. Contour interval = 0.1 e Å^{-3}. Zero and negative contours are broken and dotted, respectively.

Discussion

Figure 4a shows values of the charge density at bond CPs, ρ_b, for the bonds in the cation. The lines are the experimentally-determined bond paths between nuclear positions. The last figure ($DMANH^+_{exp}$) is the value of ρ_b found in the crystal; the first two figures (DMAN and *DMANH*$^+$) are obtained from *ab initio* MO calculations for a molecule of unprotonated DMAN by Platts *et al.*,[4] and for a molecule of protonated $DMANH^+$ as described above.

In the crystal, the proton H1nn is covalently bonded to N2. The Laplacian ($\nabla^2\rho$) value at the N2−H1nn CP is negative, but the N1−H1nn CP is in a region of positive $\nabla^2\rho$, 4.3(1) e Å^{-5} at the CP. This is typical of an ionic interaction between donor hydrogen and acceptor atom. In strong cationic [N−H···N]$^+$ bonds, the lone pair of the hydrogen-bonded nitrogen becomes strongly polarized (stretched) in the direction of the hydrogen bond; this effect is clearly seen in Figure 3a and to a lesser extent in the theoretical Laplacian distribution shown in Figure 3b. The same effect was noted in a theoretical Laplacian distribution for the proton sponge 1,6-diazabicyclo-[4.4.4]tetradecane by Howard *et al.*[5]

The [N−H···N]$^+$ bond paths are not linear (Figure 4a). This calls into question the precise meaning of one of the conventional geometrical parameters used in characterizing hydrogen bonds, namely the bond angle at the H atom. For example, the geometrical bond angle at H(1NN) is 153.3° (Table 3), whereas the angle between the bond paths is 136.2°. Further, the bond paths from H(1NN) to the adjacent N atoms are longer than the internuclear distances; for example the N(1)···H(1NN) bond path length is 1.615 Å, and the internuclear distance is 1.608 Å.

Repulsion between N1 and N2 is evident through their outward displacements relative to C1 and C8. The attractive effect of the proton apparently does not completely counteract this. There is good agreement between the ρ_b values for DMAN and *DMANH*$^+$, except, as might be expected, in the neighborhood of the hydrogen bond. These theoretical values suggest that protonation decreases the density in the C−N bonds. The $DMANH^+_{exp}$ values, however, are systematically higher than the theoretical values for $DMANH^+$, except in the C−H bonds, where they are lower.

In the anion, according to the experiment, the critical points in the strong [O−H···O]$^-$ hydrogen bond lie in regions of negative $\nabla^2\rho$ within the valence shell charge concentration (VSCC) of the H atom, reflecting some degree of apparent polarization in a direction inclined to the O···O internuclear vector, observable on the Laplacian map (Figure 3c). The hydrogen bond paths are linear, unlike those in the cation. Furthermore, the bond angle at H is close to 180°. The H atom VSCC is separated from those of the O atoms, and there appears to be an ionic interaction between H and *both* donor and acceptor oxygens. The theoretical Laplacian distribution in Figure 3d, on the other hand, shows the hydrogen atom covalently bonded to O1a. Lone pairs on the chlorine atoms clearly seen in Figure 3d are not evident in the experimental map. Presumably this is a consequence of the highly contracted κ'' values for Cl noted above.

Within experimental error, the anion is symmetrical with respect to ρ_b across a line passing midway between C2a, C3a and O1a, O4a (Figure 4b), except in the bond paths to the hydrogen atom, which carries a valence monopole charge of +0.44(2) e. The formal C═O and C−O bonds have quite similar values of ρ_b, although the formally double bonds C1a−O2a and C4a−O3a are markedly shorter [1.221(2) Å] than the formally single bonds C1a−O1a and C4a−O4a [1.283(2), 1.287(2) Å]. The experimental ellipticity values for these bonds are anomalous in that more nearly equal values (0.14, 0.17) occur for C1a−O1a, C1a−O2a than for the other $-CO_2$ group. The proton is a little closer to O1a than to O4a and one might expect the left-hand $-CO_2$ group to be more likely to show one single and one double bond than the right-hand one, in which the ellipticities are 0.02, 0.12.

The ellipticities computed from the wave function are systematically smaller but do not show this anomaly. C1a−O2a has an ellipticity of 0.09, compared with 0.00 for the

(32) Frisch, M. J.; Trucks G. W.; Head-Gordon, M.; Gill, P. M. W.; Wong, M. W.; Foresman, J. B.; Johnson, B. G.; Schlegel, H. B.; Robb, M. A.; Replogle, E. S.; Gomperts, R.; Andres, J. L.; Raghavachari, K.; Binkley, J. S.; Gonzales, C.; Martin, R. L.; Fox, D. J.; Defrees, D. J.; Baker, J.; Stewart, J. J. P.; Pople, J. A. *Gaussian 94*; Gaussian Inc.: Pittsburgh, PA, 1994.

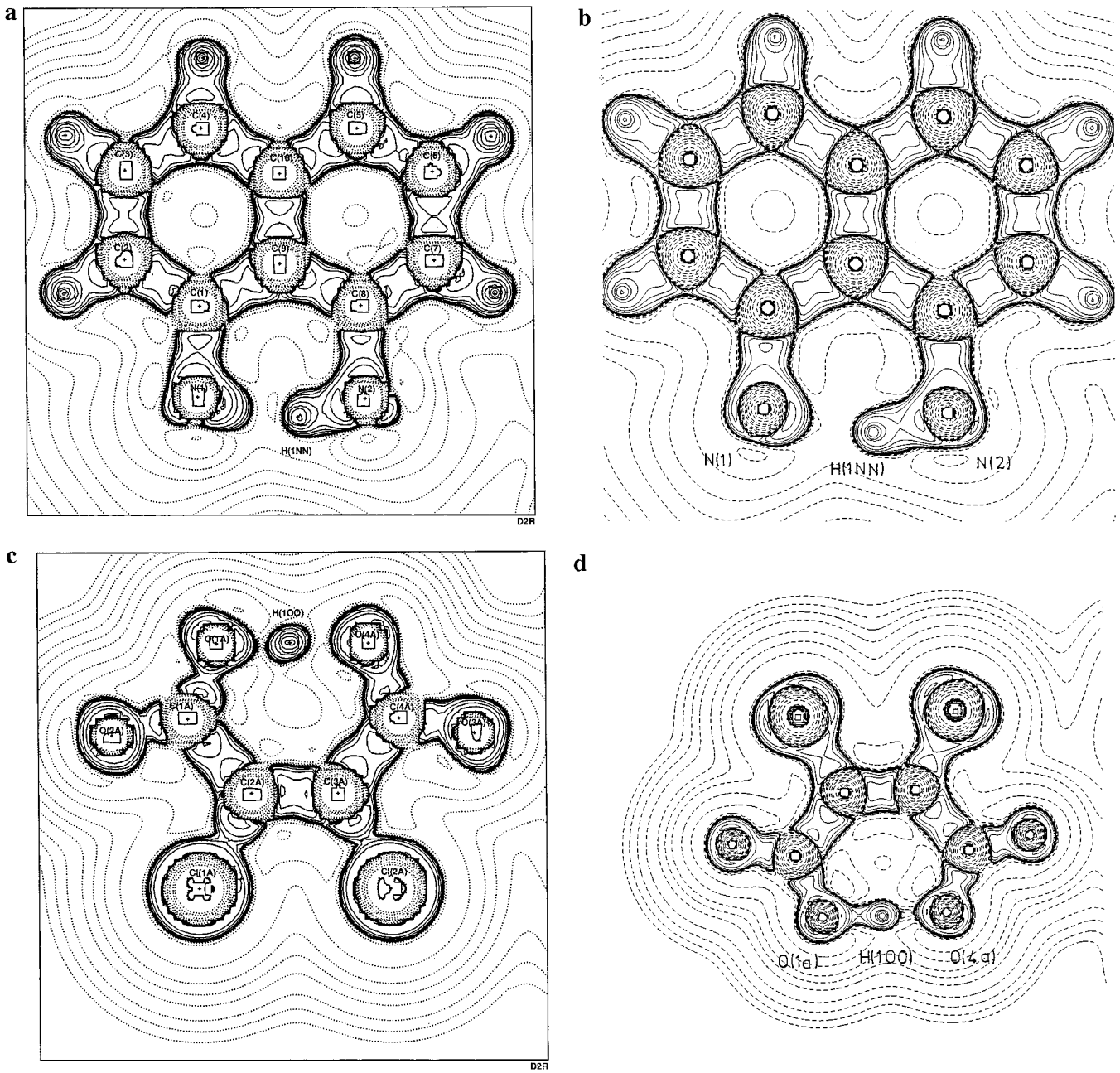

Figure 3. Laplacian maps in the plane of the cation computed from the experimental multipole populations (a) and from the *ab initio* wave function (b) and for the anion, from the experiment (c) and from the wave function (d). Contours are at logarithmic intervals in $-\nabla^2\rho$ e Å^{-5}.

formally single bond C1a−O1a. The difference between C4a−O3a (0.03) and C4a−O4a (0.00) is smaller than that for the −COOH group.

Protonation of DMAN to DMANH$^+$ causes deshielding of the outer carbons as a result of migration of charge toward the positive charge of the proton. Hence the ^{13}C solid-state NMR chemical shifts for the outer carbons increase and the difference δ(DMAN) − δ(DMANH$^+$) is negative. The monopole charges for the carbon atoms correlate with these chemical shift differences. The outer, protonated carbons are negatively charged while the inner, quaternary carbons are positively charged. This is illustrated in Figure 5; the NMR data are taken from ref 12.

Relations exist between properties at critical points in the weak hydrogen bonds (Table 3) and their geometrical parameters. For the last few years such interactions have been a subject of intensive studies,[33−48] and a recent review.[49] As a result of calculations of properties at CPs we have obtained the values of ρ_b and $\nabla^2\rho_b$ for nonbonded contacts defining stronger and weaker hydrogen bonds. A question can be asked whether

(33) Bader, R. F. W.; Tang, T.-H.; Tal, Y.; Biegler-König, F. W. *J. Am. Chem. Soc.* **1982**, *104*, 946.
(34) Boyd, R. J.; Choi, S. C. *Chem. Phys. Lett.* **1985**, *120*, 80; **1986**, *129*, 62.
(35) Steiner, T.; Saenger, W. *Acta Crystallogr.* **1994**, *B50*, 348.
(36) Braga, D.; Grepioni, F.; Sabatino, P.; Desiraju, G. R. *Organometallics* **1994**, *13*, 3532.
(37) Steiner, T. *J. Chem. Soc., Chem. Commun.* **1994**, 2341.
(38) Sharma, C. V. K.; Desiraju, G. R. *J. Chem. Soc., Perkin Trans. 2* **1994**, 2345.
(39) Steiner, T.; Saenger, W. *Carbohydr. Res.* **1995**, *266*, 1.
(40) Steiner, T. *Acta Crystallogr.* **1995**, *D51*, 93.
(41) Braga, D.; Grepioni, F.; Biradha, K.; Pedireddi, V. R.; Desiraju, G. R. *J. Am. Chem. Soc.* **1995**, *117*, 3156.
(42) Steiner, T. *J. Chem. Soc., Perkin Trans. 2* **1995**, 1315.
(43) Steiner, T.; Saenger, W. *J. Chem. Soc., Chem. Commun.* **1995**, 2087.
(44) Steiner, T.; Starikov, E. B.; Tamm, M. *J. Chem. Soc., Perkin Trans. 2* **1996**, 67.
(45) Steiner, T.; Kanters J. A.; Kroon J. *Chem. Commun.* **1996**, 1277.
(46) Desiraju, G. R. *Acc. Chem. Res.* **1996**, *29*, 441.

Table 3. Geometry of the Hydrogen Bonds in $DMANH^+ClMH^-$ Calculated from Neutron Data (D Signifies Donor, A Acceptor)

	D−H/Å	H···A/Å, symmetry	D···A/Å	DHA/deg
1	N2−H1nn	H1nn···N1	N2···N1	N2−H1nn···N1
	1.106(5)	1.608(6)	2.644(2)	153.3(5)
2	O1a−H1oo	H1oo···O4a	O1a···O4a	O1a−H1oo···O4a
	1.149(7)	1.235(7)	2.383(4)	178.5(6)
3	C11−H111	H111···O2a, 0.5 + *X*, *Y*, 2.5 − *Z*	C11···O2a	C11−H111···O2a
	1.084(4)	2.410(6)	3.118(3)	121.6(4)
4	C14−H141	H141···O2a, 0.5 + *X*, *Y*, 2.5 − *Z*	C14···O2a	C14−H141···O2a
	1.095(4)	2.535(6)	3.235(3)	120.8(3)
5	N2−H1nn	H1nn···O2a, 0.5 + *X*, *Y*, 2.5 − *Z*	N2···O2a	N2−H1nn···O2a
	1.106(5)	2.437(6)	3.055(3)	113.7(4)
6	C7−H7	H7···O3a	C7···O3a	C7−H7···O3a
	1.087(6)	2.107(7)	3.193(4)	176.1(6)
7	C14−H142	H142···O4a, −*X*, −*Y*, 2 − *Z*	C14···O4a	C14−H141···O4a
	1.096(5)	2.353(5)	3.408(3)	160.9(4)
8	C14−H141	H141···O1a, 0.5 + *X*, *Y*, 2.5 − *Z*	C14···O1a	C14−H141···O1a
	1.095(4)	2.815(5)	3.844(3)	156.6(4)
9	C14−H142	H142···O3a, −*X*, −*Y*, 2 − *Z*	C14···O3a	C14−H142···O3a
	1.096(5)	2.778(7)	3.514(4)	124.2(4)
10	C14−H143	H143···O3a	C14···O3a	C14−H143···O3a
	1.091(5)	2.570(6)	3.575(4)	152.8(4)
11	C11−H111	H111···Cl1a, 0.5 + *X*, *Y*, 2.5 − *Z*	C11···Cl1a	C11−H111···Cl1a
	1.084(4)	3.029(5)	4.028(3)	153.5(5)
12	C11−H112	H112···Cl2a, 0.5−*X*, −*Y*, *Z* − 0.5	C11···Cl2a	C11−H112···Cl2a
	1.084(5)	2.941(5)	3.654(2)	123.0(4)
13	C11−H113	H113···O4a, −*X*, −*Y*, 2 − *Z*	C11···O4a	C11−H113···O4a
	1.090(6)	2.718(6)	3.749(3)	157.7(4)
14	C11−H113	H113···O1a, −*X*, −*Y*, 2 − *Z*	C11···O1a	C11−H113···O1a
	1.090(6)	2.797(6)	3.586(3)	129.1(5)
15	C4−H4	H4···Cl1a, *X*, *Y*, *Z* − 1	C4···Cl1a	C4−H4···Cl1a
	1.099(6)	2.760(6)	3.838(3)	166.4(5)
16	C5−H5	H5···Cl1a, *X*, *Y*, *Z* − 1	C5···Cl1a	C5−H5···Cl1a
	1.100(6)	3.137(7)	4.123(3)	149.6(5)

these parameters describing properties of electron density at CPs are somehow related to the commonly accepted structural parameters for interactions such as the donor−hydrogen distances (D−H), the donor−acceptor separations (D···A), hydrogen−acceptor distances (H···A), or donor−hydrogen−acceptor angles (D−H···A), and in fact properties of the electron density at CPs have already been used to characterize different types of weak interactions,[50] and, in particular, C−H···O hydrogen bonding.[51]

It appears that for all C−H···A contacts listed in Table 3 (with the exception of three) the values of ρ_b are at least 10 times larger than their esds. In three cases from Table 3 (numbers 8, 9, and 11) we could not find any CPs for the H···A contacts. The value of ρ_b correlates very well with the neutron H···A internuclear distances, with a correlation coefficient equal to −0.97 for the seven C−H···O contacts. The shorter the H···O distance the more electron density is accumulated at the CPs for these contacts. This relationship is illustrated in Figure 6. In general such relationships between ρ_b and structural parameters characterizing a weak interaction are probably not linear ones. This seems to be the case, for example, when all types of hydrogen bonds (the strongest $[N-H\cdots N]^+$ and $[O-H\cdots O]^-$ through the weakest C−H···O type) in the complex $DMANH^+ClMH^-$ are considered on the same scale. A similar conclusion was reached on the basis of *ab initio* calculations by Alkorta and Elguero.[52]

Additionally, there is a very good correlation between ρ_b and the values of $\nabla^2\rho_b$ at CPs for weak C−H···O contacts, with the correlation coefficient equal to 0.99 for seven data points (Figure 7). This means that ρ_b and $\nabla^2\rho_b$ can carry the same information for weak C−H···O contacts. The values of $\nabla^2\rho_b$ for C−H···O contacts also correlate with the H···O internuclear distances (Figure 8; correlation coefficient −0.97).

We have carried out an *ab initio* MO calculation for a model system consisting of a benzene molecule and a formate ion, arranged to mimic the C−H···O bridged hydrogen bonding system found in the crystal (Chart 1). The 6-31G** [53] basis set supplemented with a set of anion diffuse functions[54] for the two oxygen atoms was used at the Hartree−Fock level, employing GAMESS.[55] A stable (hypothetical) complex is formed, and the values of ρ_b at the CPs located between a hydrogen atom of a benzene molecule and each oxygen atom of the ion agree well with those found in the weak C−H···O interactions in the DMAN salt. In Figure 9 we show the relationships between H···O distance and ρ_b as calculated for the model benzene/formate anion complex (data points shown as circles), and for an additive superposition of contributions to ρ_b from isolated components of the complex (data points shown as squares). These latter values were computed for the same sets of geomerical parameters as were taken for the complex.

(47) Subramanian, K.; Lakshmi, S.; Rajagopalan, K.; Koellner, G.; Steiner, T. *J. Mol. Struct.* **1996**, *384*, 121.
(48) Steiner, T.; Lutz, B.; van der Maas, J.; Veldman, N.; Schreurs, A. M. M.; Kroon, J.; Kanters, J. A. *Chem. Commun.* **1997**, 191.
(49) Steiner, T. *Chem. Commun.* **1997**, 727.
(50) Tsirelson, V. G.; Zou, P. F.; Tang, T.-H.; Bader, R. F. W. *Acta Crystallogr.* **1995**, *A51*, 143.
(51) Koch, U.; Popelier, P. L. A. *J. Phys. Chem.* **1995**, *99*, 9747.
(52) Alkorta, I.; Elguero, J. *J. Phys. Chem.* **1996**, *100*, 19367.
(53) Hehre, W. J.; Ditchfield, R.; Pople, J. A. *J. Chem. Phys.* **1972**, *56*, 2257. Ditchfield, R.; Hehre, W. J.; Pople, J. A. *J. Chem. Phys.* **1971**, *54*, 724. Harihavan, P. C.; Pople, J. A. *Theor. Chim. Acta* **1973**, *28*, 213.
(54) Frisch, M. J.; Pople, J. A.; Binkley, J. S. *J. Chem. Phys.* **1984**, *80*, 3265.
(55) Schmidt, M. W.; Baldridge, K. K.; Boatz, J. H.; Elbert, S. T.; Gordon, M. S.; Jensen, J. J.; Koseki, S.; Matsunaga, N.; Nguyen, K. A.; Su, S.; Windus, T. L.; Dupuis, M.; Montgomery, J. A. *J. Comp. Chem.* **1993**, *14*, 1347.

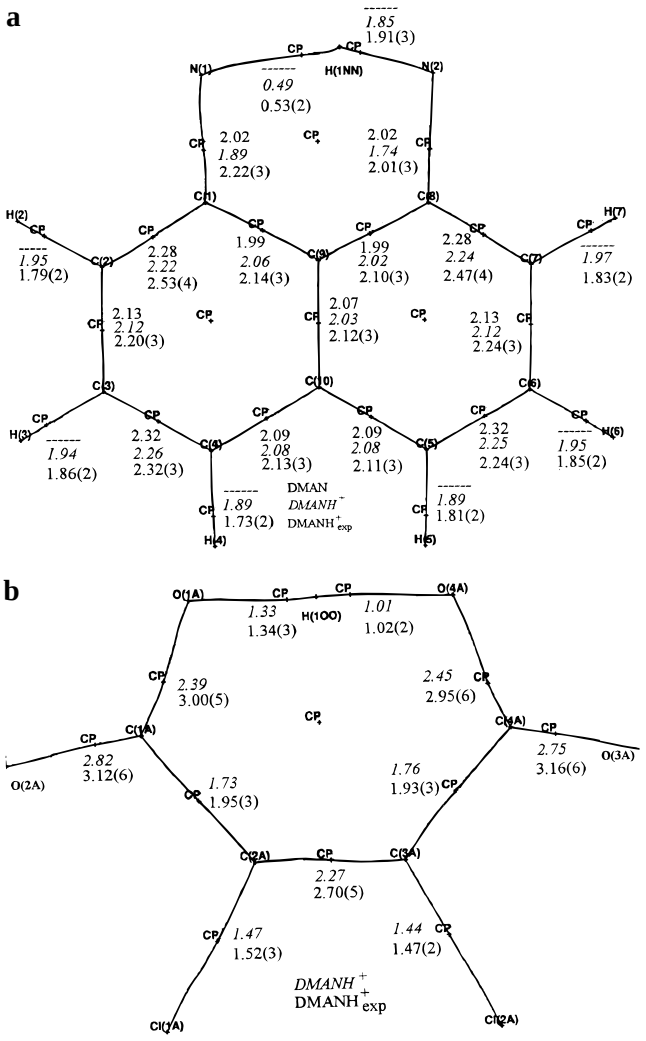

Figure 4. Bond paths (lying in the crystallographic mirror plane of the ions), showing locations of critical points, and values of ρ_b in (a) the cation ($DMANH^+_{exp}$) and (b) the anion. The values labeled DMAN and *DMANH*$^+$ are obtained from *ab initio* theoretical calculations for the free base (ref 4) and protonated base, respectively.

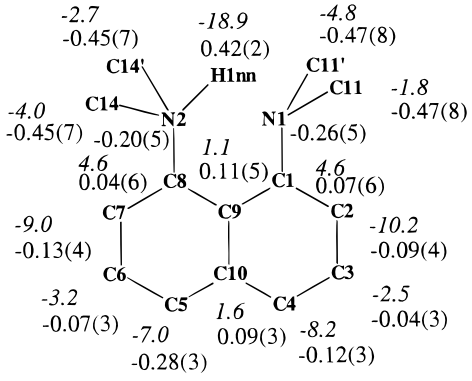

Figure 5. Chemical shift differences, δ (DMAN) − δ ($DMANH^+$) (ppm, italic values are from ref 12), and monopole charges (e).

The ρ_b values are systematically different for the complex compared to the summed fragments obtained by superposition of the benzene and formate ion densities, but the difference in ρ_b values at the equilibrium distance for the two cases is only about twice the experimental esd on ρ_b. The difference gets larger at shorter distances than the equilibrium distance. The ρ_b value is consistently smaller for the interacting case, consistent with an ionic interaction making the atomic density

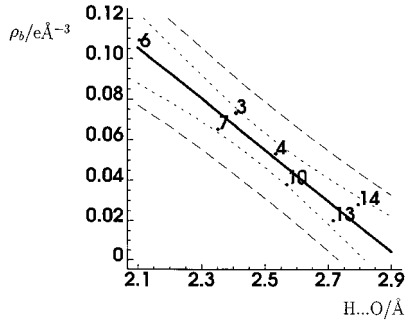

Figure 6. Plot of ρ_b *vs* H···A internuclear distance (A signifies acceptor); $\rho_b = -0.13(2)$H···A + 0.37(4); $R = -0.97$ for $n = 7$ data points.

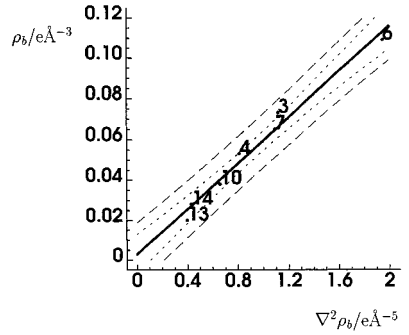

Figure 7. Plot of ρ_b *vs* $\nabla^2\rho_b$; $\rho_b = 0.056(4)\nabla^2\rho_b + 0.003(4)$; $R = 0.99$ for $n = 7$ data points.

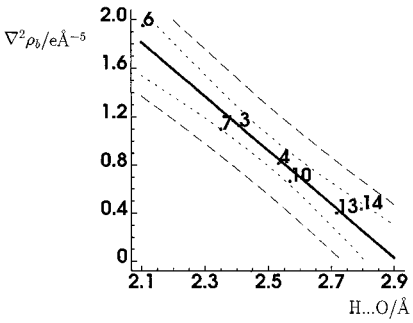

Figure 8. Plot of $\nabla^2\rho_b$ *vs* H···A internuclear distance; $\nabla^2\rho_b = -2.2(2)$H···A + 6.5(6); $R = -0.97$ for $n = 7$ data points.

Chart 1

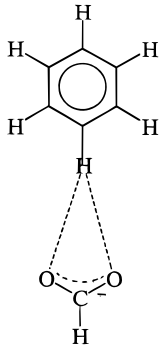

distributions contract toward the nuclei. Note that Figure 9 illustrates the nonlinear behavior of ρ_b over a range of nonequilibrium distances, whereas in Figure 6 (as previously discussed) the variation of ρ_b over a range of distances found in the crystal is linear. An almost equally good fit of ρ_b to H···O for the model system can be obtained with a Pauling bond-order type relation $\rho_b = 9.02(\text{H}\cdots\text{O})^{-5.7}$. We are grateful to one of the referees for pointing this out.

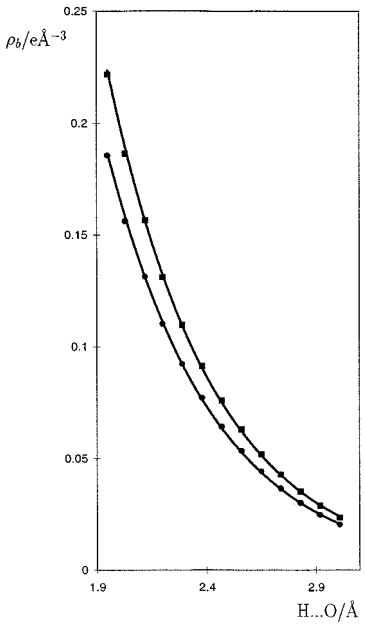

Figure 9. Plot of ρ_b *vs* H···O internuclear distance for the formate ion and benzene molecule model system (Chart 1). Data points marked by circles show ρ_b values for the complex, $\rho_b = 10.625 \exp(-2.073\text{H}\cdots\text{O})$; squares show the summed fragments, $\rho_b = 13.457 \exp(-2.102\text{H}\cdots\text{O})$.

Conclusions

This is the first experimental charge density study to explore the nature of the charged hydrogen bonds found in proton sponge complexes. The technique gives a description of properties of molecules in terms of the electron density which is more detailed than could be obtained from geometrical parameters alone. The $[Me_2N-H\cdots NMe_2]^+$ hydrogen bond in the cation is bent ($\angle N-H\cdots N = 153.5°$), also the bond paths are bent. On the basis of the shape of the bond paths it appears that this bond has multicenter character with a minor contribution from an oxygen atom (O2a) in a neighboring anion. As a result of interplay between H-bonding attractive interactions and steric repulsion between bulky NMe_2 groups, N−C(aromatic) bond paths are slightly curved, and the N atoms are pushed outward. The lone pair of this acceptor nitrogen atom is polarized in the direction of the hydrogen bond.

Ab initio theoretical ρ_b values for DMAN and $DMANH^+$ moieties differ in the neighborhood of the H-bonding site. For the $DMANH^+$ cation the experimental ρ_b values for C−C, C−N, and N−H bonds are systematically higher than the theoretical values. The H bond in the $ClMH^-$ anion is asymmetrical and almost linear in bond paths and in bond angle.

Properties at critical points appear to be useful in the description of the weakest (C−H..O) hydrogen bonds. Such weak hydrogen bonds are difficult to characterize by the use of geometrical parameters (such as donor−H···acceptor distances and angles), or by the use of thermal parameters associated with these atoms. However it is possible to obtain significant relationships between critical point properties and geometrical parameters for these bonds. The charge density distribution provides information about weak interactions which would be missed if only geometrical parameters were analyzed. The model study of the benzene···formate anion shows that the density at C-H···O hydrogen bond critical points is systematically lower than the density of the superposed moieties, but by an amount which is on the threshold of current experimental measurements analyzed with multipole-based models. It suggests that improved models (or measurements) will be required before diffraction-based charge density studies can give reliable information on such weak hydrogen bonds.

Acknowledgment. We are very grateful to Dr. S. T. Howard (University of Wales, Cardiff) for a calculation of the wave function for the DMAN salt using the EPSRC 'Columbus' computational chemistry facility, for useful discussions regarding the analysis of hydrogen bonding, and for a critical reading of the manuscript. We also thank the Department of Chemistry, University of Warsaw, for Grant No. 12-501-07-BW-1343/41/96, the UK EPSRC for a graduate studentship (for K.L.McC), and the Royal Society and the Polish Academy of Sciences for enabling P.R.M. and K.W. to participate in the European Science Exchange Programme.

Supporting Information Available: Tables of fractional atomic coordinates and anisotropic displacement parameters; monopole charges, κ' and κ'' values obtained from the refinement; critical point data; multipole population coefficients; definitions of local axes; observed and calculated structure factors; bond lengths and angles from this work and ref 20 (9 pages). See any current masthead page for ordering and Internet access instructions.

JA971940V